Efficiency-enhanced optical parametric down conversion for mid-infrared generation on a tandem periodically poled MgO-doped stoichiometric lithium tantalate chip

Y. H. Liu,[1] Z. D. Xie,[1] W. Ling,[1] Y. Yuan,[1] X. J. Lv,[1] J. Lu,[1] X. P. Hu,[1] G. Zhao,[1] and S. N. Zhu[1,*]

[1]*National Laboratory of Solid State Microstructures, College of Physics, Nanjing University, Nanjing 210093, China*
[*]*zhusn@nju.edu.cn*

Abstract: We report an efficiency-enhanced mid-infrared generation via optical parametric down conversion. A tandem periodically-poled MgO-doped stoichiometric lithium tantalate crystal is used to realize on-chip generation and amplification of mid-infrared radiation inside an optical parametric oscillator cavity. We achieved 21.2% conversion efficiency (24% slope efficiency), which is among the highest efficiencies for the pump-to-mid-infrared conversion, with 1064 nm Nd class laser pump. The maximum average output power at 3.87μm reached 635 mW with a 3.0 W pump.

©2011 Optical Society of America

OCIS codes: (140.3070) Infrared and far-infrared lasers; (190.4970) Parametric oscillators and amplifiers; (190.4223) Nonlinear wave mixing.

References and links

1. R. Guoguang and H. Yunian, "Laser-based IRCM system defenses for military and commercial aircraft," Laser Infrared **36**, 1–6 (2006).
2. Y. Peng, W. Wang, X. Wei, and D. Li, "High-efficiency mid-infrared optical parametric oscillator based on PPMgO:CLN," Opt. Lett. **34**(19), 2897–2899 (2009).
3. M. E. Dearborn, K. Koch, G. T. Moore, and J. C. Diels, "Greater than 100% photon-conversion efficiency from an optical parametric oscillator with intracavity difference-frequency mixing," Opt. Lett. **23**(10), 759–761 (1998).
4. J. M. Fraser and C. Ventalon, "Parametric cascade downconverter for intense ultrafast mid-infrared generation beyond the Manley-Rowe limit," Appl. Opt. **45**(17), 4109–4113 (2006).
5. K. Koch, G. T. Moore, and E. C. Cheungy, "Optical parametric oscillation with intracavity difference-frequency mixing," J. Opt. Soc. Am. B **12**(11), 2268–2273 (1995).
6. G. T. Moore and K. Koch, "Efficient High-Gain Two-Crystal Optical Parametric Oscillator," IEEE J. Quantum Electron. **31**(5), 761–768 (1995).
7. A. Berrou, J.-M. Melkonian, M. Raybaut, A. Godard, E. Rosencher, and M. Lefebvre, "Specific architectures for optical parametric oscillators," C. R. Phys. **8**(10), 1162–1173 (2007).
8. K. J. McEwan and J. A. C. Terry, "A tandem periodically-poled lithium niobate (PPLN) optical parametric oscillator (OPO)," Opt. Commun. **182**(4-6), 423–432 (2000).
9. J. M. Fukumoto, H. Komine, W. H. Long, Jr., and E. A. Stappaerts, "Periodically Poled $LiNbO_3$ Optical Parametric Oscillator with Intracavity Difference Frequency Mixing," in: W. R. Bosenberg, M. M. Fejer (Eds.), Advanced Solid State Lasers, OSA Trends in Optics and Photonics Series, **19**, 245–248 (1998).
10. H. C. Guo, Y. Q. Qin, Z. X. Shen, and S. H. Tang, "Mid-infrared radiation in an aperiodically poled $LiNbO_3$ superlattice induced by cascaded parametric processes," J. Phys. Condens. Matter **16**(47), 8465–8473 (2004).
11. G. Porat, O. Gayer, and A. Arie, "Simultaneous parametric oscillation and signal-to-idler conversion for efficient downconversion," Opt. Lett. **35**(9), 1401–1403 (2010).
12. N. E. Yu, S. Kurimura, Y. Nomura, M. Nakamura, K. Kitamura, J. Sakuma, Y. Otani, and A. Shiratori, "Periodically poled near-stoichiometric lithium tantalate for optical parametric oscillation," Appl. Phys. Lett. **84**(10), 1662–1664 (2004).
13. W. L. Weng, Y. W. Liu, and X. Q. Zhang, "Temperature-Dependent Sellmeier Equation for 1.0 mol% Mg-Doped Stoichiometric Lithium Tantalate," Chin. Phys. Lett. **25**(12), 4303–4306 (2008).
14. S. N. Zhu, Y. Y. Zhu, Z. Y. Zhang, H. Shu, H. F. Wang, J. F. Hong, C. G. Ge, and N. B. Ming, "$LiTaO_3$ crystal periodically poled by applying an external pulsed field," J. Appl. Phys. **77**(10), 5481–5483 (1995).

#149782 - $15.00 USD Received 23 Jun 2011; revised 6 Aug 2011; accepted 7 Aug 2011; published 22 Aug 2011
(C) 2011 OSA

15. X. P. Hu, X. Wang, J. L. He, Y. X. Fan, S. N. Zhu, H. T. Wang, Y. Y. Zhu, and N. B. Ming, "Efficient generation of red light by frequency doubling in a periodically-poled nearly-stoichiometric $LiTaO_3$ crystal," Appl. Phys. Lett. **85**(2), 188–190 (2004).

1. Introduction

Mid-infrared (mid-IR) radiation around $3.8\mu m$ is of interest for a number of demanding applications, such as gas spectroscopy, environmental monitoring, atmospheric sensing, biomedical, and mid-IR countermeasures [1, 2]. One of the most widely-used scheme for mid-IR generation is by using the optical parametric down conversion, where a pump photon with higher frequency ω_p splits into two photons with lower frequencies ω_s and ω_i called signal and idler, respectively. However, when pumped by the most sophisticated Nd class solid state lasers at around 1064 nm, the power of idler light in the mid-IR range is limited by the low splitting ratio from the pump photon, i.e., the conversion efficiency is theoretically limited to about 1/4 even at 100% quantum efficiency [3, 4]. To increase the pump-to-mid-IR conversion efficiency, the pump lasers with lower frequencies may be used, but the performances of these lasers still need to be improved for high power applications. On the other hand, the efficiency can also be improved by extracting the residual energy from the signal light. For example, by using a cascaded optical parametric oscillator-optical parametric amplifier (OPO-OPA) process, it is possible to use the signal to amplify the idler. In the first section, the mid-IR light is generated in a similar way as the standard OPO; in the second section, the signal is used as pump to further amplify the existing mid-IR light. This method has been discussed as theoretical possibility [5–7] and experimentally demonstrated by using two independent nonlinear crystals with both synchronous [3, 6, 8] and Q-switched laser operating at 20 Hz repetition rate [9] pumping schemes. Later people found the OPO-OPA can be realized with better efficiency in a simpler setup by using a monolithic quasi-phase-matching material with complex domain structures, such as aperiodic and quasi-periodic structures [10, 11]. 14.58% pump-to-mid-IR conversion efficiency has been reported and 16.6% improvement has been achieved compared to a standard OPO.

In this letter, we present an intra-cavity OPO-OPA by a single tandem periodically-poled MgO-doped stoichiometric lithium tantalate (TPPMgSLT) crystal with two cascaded domain sections. These two sections are cascaded arranged and designed to compensate for the phase mismatching for the OPO and OPA processes, respectively. No complex domain structures are involved in this case, which simplifies the manufacturing processes. 21.2% pump-to-mid-IR conversion efficiency is obtained and it shows 77.6% efficiency enhancement compared to a single OPO. This value is among the highest efficiencies of mid-IR generation presented to date, using parametric down conversion approach with 1064 nm laser pump [2, 11, 12].

2. Method

To realize the phase matching for the OPO-OPA process, momentum conservation conditions for the OPO and OPA processes should be fulfilled simultaneously with the existences of the reciprocals of the two sections of the TPPMgSLT:

$$\Delta k_{OPO} = k_p - k_s - k_i - G_{OPO} = 0 \tag{1}$$

$$\Delta k_{OPA} = k_s - k_{s2} - k_i - G_{OPA} = 0 \tag{2}$$

where k_p, k_s, k_i are the wave vectors of the pump ω_p, signal ω_s, idler ω_i, and $G_{OPO} = \frac{2\pi}{\Lambda_{OPO}}$ is the reciprocal vector for the OPO; k_{s2} and $G_{OPA} = \frac{2\pi}{\Lambda_{OPA}}$ are the idler (ω_{s2}) wave vector and the reciprocal vector for the OPA, respectively. Λ_{OPO} and Λ_{OPA} are the poling periods of the OPO and OPA stages, respectively. According to the temperature-dependent Sellmeier equation of the 1.0 mol% MgO-doped stoichiometric lithium tantalate

#149782 - $15.00 USD Received 23 Jun 2011; revised 6 Aug 2011; accepted 7 Aug 2011; published 22 Aug 2011
(C) 2011 OSA

crystal (MgO:SLT) [13], we chose the poling periods $\Lambda_{OPO} = 28.83\mu m$ and $\Lambda_{OPA} = 31.59\mu m$ for the two stages in the following OPO-OPA process:

$$\text{OPO}: \ 1.064\mu m \rightarrow 1.47\mu m + 3.87\mu m \tag{3}$$

$$\text{OPA}: \ 1.47\mu m \rightarrow 3.87\mu m + 2.37\mu m \tag{4}$$

In these two stages, the phase matching curves of the OPO and OPA processes can be calculated from Eqs. (1) and (2). As shown in Fig. 1, the phase matching for the OPO-OPA process occurs at the cross-over point for the two curves of around $145°C$, which is measured to be $120°C$ in the experiment. The difference between them is mainly due to the inaccuracies of the Sellmeier equation and the thermal expansion of the TPPMgSLT crystal. The angular separation of the temperature tuning curves for the OPO and OPA processes is small, and therefore a wide phase-matching bandwidth for the OPO-OPA can be expected, which is calculated to be about $100°C$.

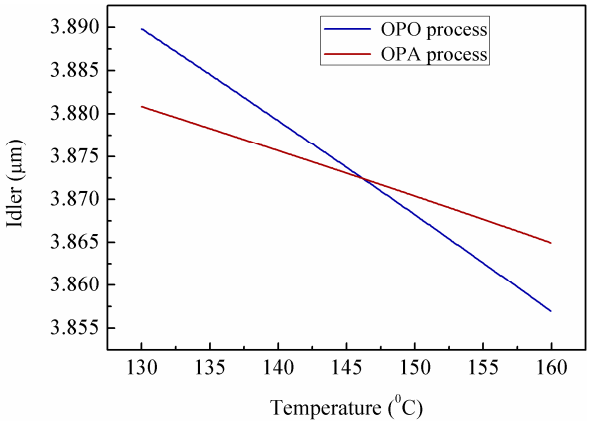

Fig. 1. The calculated phase-matching curves for the OPO and OPA processes.

Taking the plane-wave and the slowly varying envelope approximations, the parametric interaction between the amplitudes can be described by the coupling equations, under the perfect phase matching condition.

$$\begin{aligned}
\frac{dA_p(z)}{dz} &= i\kappa_{OPO}A_s(z)A_i(z) \\
\frac{dA_s(z)}{dz} &= i\kappa_{OPO}A_p(z)A_i^*(z) + i\kappa_{OPA}A_i(z)A_{s2}(z) \\
\frac{dA_i(z)}{dz} &= i\kappa_{OPO}A_p(z)A_s^*(z) + i\kappa_{OPA}A_s(z)A_{s2}^*(z) \\
\frac{dA_{s2}(z)}{dz} &= i\kappa_{OPA}A_s(z)A_i^*(z)
\end{aligned} \tag{5}$$

in Eq. (5), $\kappa_{OPO} = \frac{d_{eff}}{c}\sqrt{\frac{\omega_p\omega_s\omega_i}{n_p n_s n_i}}$ and $\kappa_{OPA} = \frac{d_{eff}}{c}\sqrt{\frac{\omega_{s2}\omega_s\omega_i}{n_{s2} n_s n_i}}$ are the coupling coefficient, in which c is the vacuum light velocity. A_j, n_j are the amplitudes, and refractive indices of $\omega_j (j = p, s, i, s2)$, respectively. $d_{eff} = 0.637d$ is the effective second order nonlinear coefficient, where $d = \frac{\chi^{(2)}}{2}$.

#149782 - $15.00 USD Received 23 Jun 2011; revised 6 Aug 2011; accepted 7 Aug 2011; published 22 Aug 2011
(C) 2011 OSA

3. Fabrication of the TPPMgSLT and experimental setup

The TPPMgSLT is fabricated using the electrical poling technique at room temperature from a 1 mm thick MgO:SLT wafer [14]. It is known that MgO:SLT, with large d_{eff}, shows high damage threshold, high resistance to the photorefractive effect, high thermal conductivity, and low IR absorption, especially compared to the commonly used lithium niobate. Furthermore the nonstoichometric defect is significantly reduced in MgO:SLT, and therefore it leads to a reduction of coercive field by ~1 order of magnitude and facilitates the electrical poling of large aperture crystals with a good uniformity of domain structures. These characteristics collectively make MgO:SLT a promising material for the high efficiency frequency conversions at high power levels. Owing to the high intracavity power density inside a high-Q OPO cavity and the advantage of MgO:SLT, high efficiency can be expected. As shown in Fig. 2, the width of OPO section is 2 mm wider than the OPA section so that we can independently test the single OPO operation. The TPPMgSLT has the lengths of 24 mm and 19 mm for the OPO and OPA sections, respectively. And the total length of the crystal is about 44 mm. The two end faces are optically polished and coated for antireflection at 1064, 1400-1500, and 3800-4200 nm. The crystal is embedded in an oven whose temperature is controlled with accuracy of $\pm 0.1°C$ for stable operation.

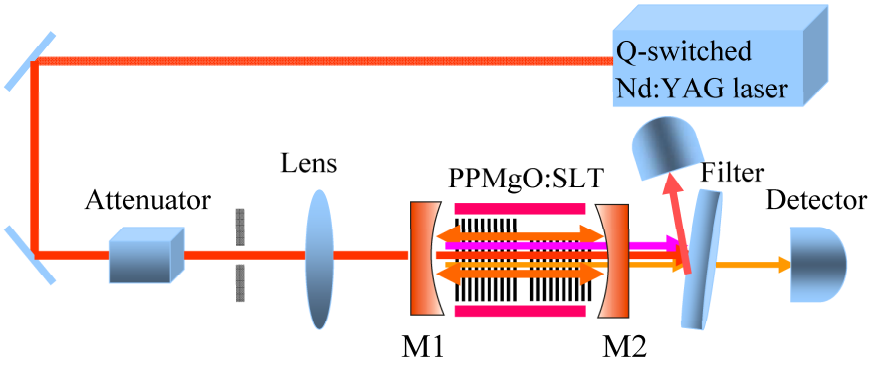

Fig. 2. Schematic of the experiment setup.

The OPO-OPA apparatus is schematically shown in Fig. 2. We use a 100-mm-long linear OPO cavity, with concave cavity mirrors M1 and M2 of 100 mm radius. Both of them are high-reflection coated (R>99%) for 1400-1500 nm to provide high-Q singly resonance for the signal, anti-reflection coated for 3800-4000 nm and anti-reflection coated for 1064 nm and 1650 nm to reduce unwanted resonances. The pump light is from a diode-pumped Nd:YAG laser working at 1064 nm, with repetition rate of 5 kHz and pulse duration of 40 ns. The pump beam is focus onto the crystal with a beam diameter of $200\mu m$, and it matches well with the waist of the cavity mode that is calculated to be $180\mu m$. A high-pass filter is used to split the pump and idler beams for the measurements.

4. Experimental results and discussion

We first characterized the OPO process while only the OPO section was illuminated by the pump beam. As shown in Fig. 3, a conversion efficiency of 12% and a slope efficiency of 14.5% could be calculated, that was 43.6% of quantum-limited performance. The oscillation started with a threshold below 500 mW and we obtained the maximum output power of 360 mW with 3 W pump. The thresholds for the pump power density of OPO and OPO-OPA processes could be calculated by solving the coupling Eq. (5), $I_{pt} = \dfrac{\varepsilon_0 n_p n_s n_i c^3}{4 d^2 \omega_s \omega_i L^2}(1 - R_s)$, where R_s and L were the equivalent reflectivity of the signal light and the length of the OPO

#149782 - $15.00 USD Received 23 Jun 2011; revised 6 Aug 2011; accepted 7 Aug 2011; published 22 Aug 2011
(C) 2011 OSA

section, respectively. The measured threshold power densities of the two processes were about 4 MW/cm^2, which were on the same order of calculated values of 1.5 MW/cm^2.

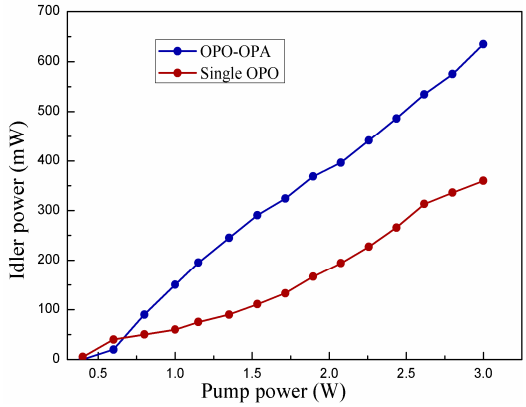

Fig. 3. Measured mid-IR output power of the single OPO and the OPO-OPA versus pump power at $120°C$.

Later, we moved the transverse position of TPPMgSLT so that the OPA section could take part in the nonlinear interaction. The temperature dependence of OPA was shown in Fig. 4, bymeasuring the output power of ω_{s2} . The measured FWHM bandwidth of OPO-OPA process was about $50°C$, which was resulted from the broad phase-matching bandwidth as discussed in section 2.

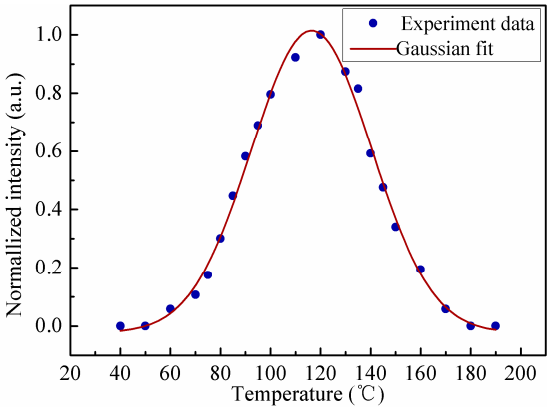

Fig. 4. Normalized output power for ω_{s2} as a function of temperature.

At the phase matching temperature of $120°C$, we measured the spectrum of the outputs using a spectrum analyzer (ANDO AQ-6315A). As shown in Fig. 5, the peaks at 1468 nm and 1187 nm were for ω_s and the second harmonic of ω_{s2} , respectively. From that, we could easily calculate the wavelengths of ω_{s2} and ω_i to be 2374 nm and 3847 nm respectively, which agreed well with the designed values in Eqs. (3) and (4). The output at other wavelength could not be recorded because of the limited response range of the spectrum analyzer. We also measured the dependence of mid-IR output power on pump power (Fig. 3). The OPO-OPA showed a similar threshold as the single OPO, but with much higher slope efficiency due to the existence of intracavity OPA process. When the pump power reached 3 W, the measured power of idler was 635 mW. The conversion and slope efficiencies for mid-IR light were 21.2% and 23.52%, respectively. Compared to the single OPO, the OPO-OPA presented 76.4% improvement on the conversion efficiency and 65.6% improvement on the

#149782 - $15.00 USD Received 23 Jun 2011; revised 6 Aug 2011; accepted 7 Aug 2011; published 22 Aug 2011
(C) 2011 OSA

slope efficiency. The improvement was attributed to the extra gain in the OPA process. The high intensity signal light could be generated inside the high-Q OPO cavity, which served as pump of OPA process in the same cavity. According to the last formula of Eq. (5), the gain of OPA could be given by:

$$g = \kappa_{OPA} |E_s| \tag{6}$$

where E_s was the electric field of the signal light in the condition of steady state. The gain of OPA process could be calculated about $g = 0.6\,\mathrm{cm}^{-1}$ from Eq. (6), which was measured to be $g = 0.5\,\mathrm{cm}^{-1}$ in a well agreement.

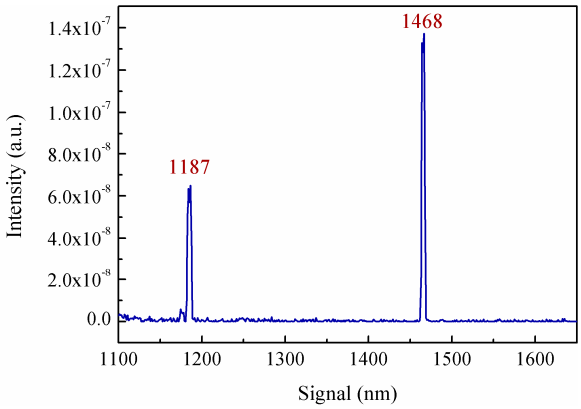

Fig. 5. Output spectrum at $120°C$ for the OPO-OPA device. The spectrum range is limited from 350 nm to 1750 nm by the spectrum analyzer.

5. Conclusion

In conclusion, we have demonstrated an efficiency enhanced mid-IR generation based on OPO-OPA using TPPMgSLT. A maximum conversion efficiency of 21.2% has been achieved, which corresponds to 77% of the quantum-limited (27.5%) performance for this pulsed OPO-OPA setup. The monolithic TPPMgSLT crystal has presented high efficiency and high intracavity power density capability and low loss for high-Q resonance in the OPO cavity. These features are also important for the future CW OPO-OPA devices and near quantum-limited performance could be expected. In this work, the pump laser has a maximum output power of about 3 W, corresponding to a power density of 45 MW/cm^2 in the experiment, which is much lower than the damage threshold of the MgO:SLT [12, 15]. Therefore, by replacing the pump source with higher power and TPPMgSLT with larger optical aperture, the OPO-OPA scheme can be readily scaled for higher power mid-IR output with high efficiency.

Acknowledgment

This work was supported by the National Natural Science Foundations of China (Nos. 11021403, 10904066 and NSAF10776011), and the State Key Program for Basic Research of China (Nos. 2011CBA00205 and 2010CB630703).

#149782 - $15.00 USD Received 23 Jun 2011; revised 6 Aug 2011; accepted 7 Aug 2011; published 22 Aug 2011
(C) 2011 OSA